Mathematical and Computer Modelling 55 (2012) 1021–1033

Contents lists available at SciVerse ScienceDirect

Mathematical and Computer Modelling

journal homepage: www.elsevier.com/locate/mcm

A modeling study of school closure to reduce influenza transmission: A case study of an influenza A (H1N1) outbreak in a private Thai school

Charin Modchang [a,e,1], Sopon Iamsirithaworn [b], Prasert Auewarakul [c], Wannapong Triampo [a,d,e,*]

[a] Biophysics Group, Department of Physics, Faculty of Science, Mahidol University, Rama VI, Bangkok 10400, Thailand
[b] Bureau of Epidemiology, Department of Disease Control, Ministry of Public Health Tivanond Road, Nonthaburi 11000, Thailand
[c] Department of Microbiology, Faculty of Medicine, Siriraj Hospital, Mahidol University, Bangkok 10700, Thailand
[d] Center of Excellence for Vectors and Vector-Borne Diseases, Faculty of Science, Mahidol University, Rama VI, Bangkok 10400, Thailand
[e] ThEP Center, CHE, 328 Si Ayutthaya Road, Bangkok 10400, Thailand

ARTICLE INFO

Article history:
Received 4 August 2010
Received in revised form 12 September 2011
Accepted 13 September 2011

Keywords:
Non-pharmaceutical intervention
SEIR model
Control measures
Bangkok

ABSTRACT

The A/H1N1 influenza pandemic has been in the spotlight since the virus was first detected in Mexico in early 2009. To prevent the repetition of the 1918 influenza pandemic, the global response to this pandemic has been strong. In Thailand and in many other countries, schools have been a major source of outbreaks, which then spreads to the general population. Understanding the dynamics of school outbreaks and the impact of disease intervention in school settings is crucial for the effective mitigation of a pandemic. Using data from outbreaks in School G, a private school in Bangkok where detailed epidemiological data were collected, we estimated the basic reproduction number (R_0) to be 3.58 [95% confidence interval: 2.88 to 4.28]. We then modeled outbreaks in school settings with Susceptible-Exposed-Infectious-Recovered (SEIR) equations and tested various interventions such as school closure and student screenings. We found that closing the school on the date with the peak number of daily incidences usually appeared to be effective in preventing further outbreaks. However, if the school was closed too early, subsequent cases would appear after reopening. With no intervention, the number of total cases reaches 83%. Individual student screenings appeared to reduce the number of total cases by up to 40%. In a situation in which the widespread outbreak of a mild disease is unavoidable and in which the goal is to slowly reach sufficient herd immunity while minimizing the number of cases, closing the school at the predicted date with the peak number of daily incidences and screening for respiratory symptoms appear to be the most appropriate intervention methods.

1. Introduction

A number of intervention strategies can reduce the impact of influenza pandemics like the 2009 A/H1N1 influenza pandemic [1–5]. Pharmaceutically, influenza vaccination can be used to reduce death and disease. However, such vaccines are unlikely to be available in a timely manner or in sufficient quantities to eradicate a pandemic [6–9]. Other non-pharmaceutical disease control options also need to be considered, such as social distancing, avoiding the use of public

* Corresponding author at: Biophysics Group, Department of Physics, Faculty of Science, Mahidol University, Rama VI, Bangkok 10400, Thailand. Tel.: +662 441 9816x1131; fax: +662 441 9322.
E-mail addresses: scharin@mahidol.ac.th (C. Modchang), iamsiri@yahoo.com (S. Iamsirithaworn), sipaw@mahidol.ac.th (P. Auewarakul), wtriampo@gmail.com, scwtr@mahidol.ac.th (W. Triampo).
1 Tel.: +662 201 5775; fax: +662 354 7159.

0895-7177/$ – see front matter © 2011 Elsevier Ltd. All rights reserved.
doi:10.1016/j.mcm.2011.09.027

transportation, wearing face masks, and closing schools to protect people from illness and to maintain critical societal functions [10–12].

Because non-pharmaceutical-based strategies have not been as extensively studied or followed up, we were motivated to research a school closure strategy that could alleviate most influenza epidemics. It has been shown that nonmedical interventions such as school closure and social isolation was beneficial in reducing the transmission of the 2009 A/H1N1 influenza, even though quantifying this benefit is not possible, and school closures are not always recommended by the World Health Organization (WHO) [2,3].

What is the effectiveness of school closure interventions against pandemic influenza? When should schools be closed? For how long should schools be closed? These are crucial questions that need to be answered. However, arriving at an optimal scheme for answering these questions is not an easy task during an actual epidemic. During the epidemic period, the epidemic curve is usually unknown, and unexpected outbreaks can occur, especially in situations involving an emerging disease. For example, one could suggest that a school should close when the absentee rate is around 15%. But an underestimation of cases could occur due to the omission of asymptomatic infected individuals. Another potential concern involves the lack of real-time or up-to-date data reports from schools, which could occur if schools lack reliable staff or are worried about how closures could impact their reputation and budgets.

As the number of confirmed cases of the A/H1N1 influenza pandemic increased globally in 2009, the United States mainly targeted students in elementary and high schools for prevention. New York's St. Francis Preparatory School closed when 28 cases of the 2009 A/H1N1 influenza pandemic were confirmed. Meanwhile, Japan swiftly acted to contain the disease through school closures and other social distancing measures [13]. Australia also responded aggressively, closing schools in Victoria and Queensland for varying periods of time. In Thailand, the Department of Disease Control confirmed numerous cases of the 2009 A/H1N1 influenza among middle school students during the early pandemic [14,15] and recommended the routine screening and isolation of cases. The schools could temporarily close if there were significant numbers of confirmed cases of the 2009 A/H1N1 influenza and if it rapidly spread through the school. The duration of a particular closing was dependent on ongoing epidemiological incidents in the affected school and on consultations with local and state health departments. Normally, a period of 5–14 days passed before the schools considered reopening.

Improving the efficacy of predictions has been the main focus in developing a mathematical model. However, our knowledge related to school closure via mathematical models has been quite limited mainly because empirical data are still relatively rare and because previous models cannot investigate how and when to close schools (for example, is closing only the infected room or floor better than closing the entire school? What is the optimum time to implement strategies?) [1,10–12]. There are many epidemic-related software packages that use school closure as one of their non-pharmaceutical interventions; e.g., InfluSim [16,17] and EpiSimS [18]. However, none of these software packages tells us how or when we should close a school to make the school closure intervention most effective. Recently, Lee et al. [19] employed an agent-based computer simulation model (ABM) to explore the effects of various school closure strategies on mitigating influenza epidemics. They found that for school closure strategies, closing schools for 8 weeks could reduce the attack rate (AR) from 35% to 25% for $R_0 = 1.4$, and durations of less than 8 weeks had little impact on the overall AR, while durations of 2 weeks or less actually slightly increased the overall AR. In their study, students that were isolated from their schools could still make contact with and spread the disease to other individuals in their communities, and this might be the reason why closing schools for 2 weeks or less slightly increased the overall AR. House et al. [20] also investigated the impact of localized short-duration school closures in England. By using a standard age-structured epidemic model, they found that relatively short duration school closures (less than or equal to 4 weeks) reduce the peak incidence by between 30% and 70% and that the closures should be carefully timed to start just before the expected epidemic peak. However, House et al. [20] did not investigate the effects of isolating sick students. Lee et al. [19] also did not study the effect of combining strategies (e.g., isolation + school closure) or partial school closures in which only some rooms or classes are closed. If we could isolate schools and students from their communities and quarantine infected students to their homes until they recover, how much more effective would the school closure and student isolation strategies be? It is interesting to address these questions. In our current study, to keep our model as simple as possible and able to run on a modern PC without the need for a supercomputer or computer cluster, we employed the SEAIR model as an efficient numerical tool for simulating school closures to investigate what is the most effective criterion for taking such a measure. It should be mentioned once again that for the model to provide precise predictions, data validation and more accurate ways of measuring data from the 2009 A/H1N1 influenza pandemic cases are needed. However, this study will certainly help scientists and mathematical modelers give better information to health officials so that they can make the right decisions when managing a pandemic.

In our work, we built a detailed school model that particularizes to the schoolroom level. This model allows us to study several intervention strategies related to an epidemic at a school, including individual room closure, individual floor closure, full school closure, and the individual screening of infectious students. Our main objective was to establish criteria for performing intervention strategies that could mitigate the 2009 A/H1N1 influenza transmission in a school and could be applied to another epidemic wave or other epidemics. We investigated the effects of starting conditions, the effectiveness of individual screenings, and the duration of closure periods on mitigating the impact of the influenza. In addition, some parameters (such as reproduction number, contact matrix, and asymptomatic ratios) that normally play significant roles in the spreading of the disease were either obtained from the empirical data or from a numerical estimation. A good estimate of the epidemic rate or parameters is needed to make the model more realistic and to provide predictions that can help healthcare planners decide the appropriate measures to take to contain infections.

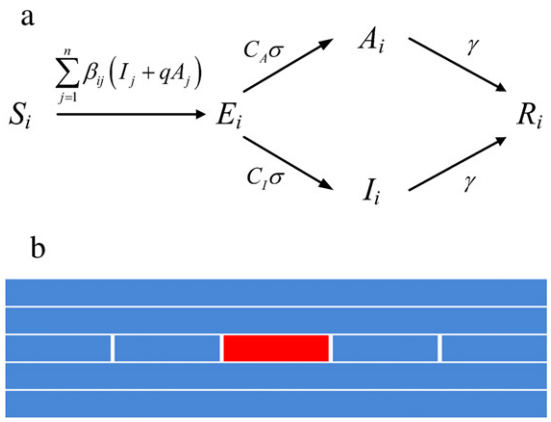

Fig. 1. (a) Model structure. S_i, E_i, I_i, A_i, and R_i represent the number of susceptible, exposed, symptomatic infectious, asymptomatic infectious, and recovered individuals in the ith compartment, respectively. Transition rate for each state is shown near the transition arrow. (b) School structure. The typical school size in Thailand is 5 floors with 5 rooms each. Each room holds approximately 50 students. The index-case room is labeled in red. The index-case floor is modeled by using a finer scale and a coarser scale on other floors.

2. Methods

2.1. The model

We developed a spatial compartment model based on traditional Susceptible-Exposed-Infectious-Recovered (SEIR) equations, where each room or floor is represented by a spatial compartment. S_i, E_i, I_i, and R_i represent the number of susceptible, exposed, symptomatic infectious, and recovered individuals in the ith compartment, respectively. Because the number of asymptomatic infectious individuals is crucial in determining the intervention strategies needed for epidemic control (see below), we separated out a number of asymptomatic individuals and represented them by the variable A_i.

We shall refer to the model as a SEAIR model. Each spatial compartment is thus governed by the same SEAIR dynamics as shown in Fig. 1(a). Susceptible individuals S_i are infected at a rate of $\sum_{j=1}^{n}\beta_{ij}(I_j + qA_j)$, where β_{ij} is the transmission rate from the jth compartment to the ith compartment, which incorporates the encounter rate between susceptible and infectious individuals together with the probability of transmission. q is the asymptomatic infectiousness, which accounts for the "average" reduction in transmissibility among individuals in the asymptomatic class (A) [21,22]. The transmission rates between these compartments are proportional to the contact rates and are scaled such that the model yields a given basic reproduction number R_0 [23]. The summation is taken over all of the compartments that can spread the infection to the ith compartment. The infected individuals (E_i) incubate the infection for a mean duration of $1/\sigma$. After passing through the exposed state, infected individuals become fully contagious, and a fraction (C_I) of them develops clinical symptoms (I_i), while the remainder (C_A) becomes asymptomatic (A_i) ($C_A + C_I = 1$). The mean duration of the contagious stage for both symptomatic and asymptomatic groups is assumed to be $1/\gamma$. Finally, the infectious individuals develop protective immunity and are added to the recovered group (R_i).

Based on the described model and the structure seen in Fig. 1, the law of mass action leads to the following set of deterministic coupled ordinary differential equations:

$$\frac{dS_i}{dt} = -S_i \sum_{j=1}^{n} \beta_{ij}(I_j + qA_j) \tag{2.1}$$

$$\frac{dE_i}{dt} = S_i \sum_{j=1}^{n} \beta_{ij}(I_j + qA_j) - \sigma E_i \tag{2.2}$$

$$\frac{dA_i}{dt} = C_A\sigma E_i - \gamma A_i \tag{2.3}$$

$$\frac{dI_i}{dt} = C_I\sigma E_i - \gamma I_i \tag{2.4}$$

$$\frac{dR_i}{dt} = \gamma A_i + \gamma I_i \tag{2.5}$$

where $i = 1, 2, \ldots, n$, and n is the number of spatial compartments. These equations describe the rate of change of susceptible, exposed, asymptomatic infectious, symptomatic infectious, and recovered individuals, respectively, in the ith

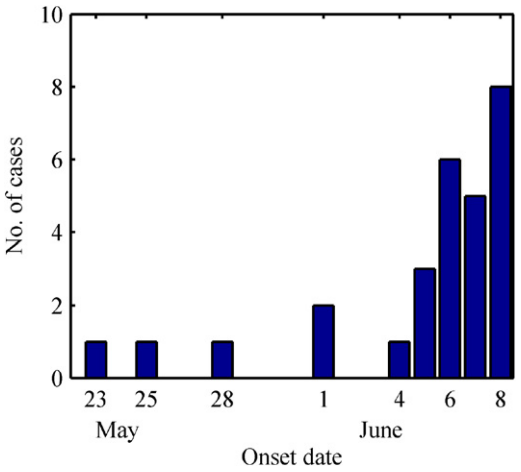

Fig. 2. Number of daily laboratory-confirmed cases of the novel H1N1 in school *G*. Note that in this figure only the early exponential growth phase is shown.

spatial compartment, with the conservation constraint $S_i + E_i + A_i + I_i + R_i = N_i$, where N_i is the total number of students in the ith compartment. Here, the assumption of a homogeneous well-mixed population has been made.

For the sake of simplicity, we used the school structure shown in Fig. 1(b) as the study example. A typical medium-sized school in Thailand has 5 floors with 5 rooms each and about 50 students in each room. For illustrative purposes, we assumed that the index-case room (i.e., the room that we found the first symptomatic infectious student) was the room located at the center of the school (labeled in red). In the index-case floor, we used a finer scale by modeling each room as a compartment. However, for quick calculations, we modeled the other floors by using a coarser scale by grouping 5 rooms into a compartment. In total, we had 9 spatial compartments that could interact with each other via a contact matrix $\mathbf{M} = [m_{ij}]$. The elements of the transmission matrix $\boldsymbol{\beta} = [\beta_{ij}]$ were proportional to the elements in this contact matrix [23].

We based our parameter values on epidemiological data and the seasonal influenza and 2009 influenza A (H1N1) estimates that were commonly reported in the literature. These parameter values were a mean incubation period $(1/\sigma)$ of 2 days, and a mean infectious period $(1/\gamma)$ of 5 days. However, uncertainty remains concerning the key epidemiological parameters of influenza A (H1N1), namely, the basic reproduction number R_0. The first report of R_0 was made by Fraser et al., who estimated the basic reproduction number R_0 of the Mexican outbreak of H1N1 to be in the range of 1.2–1.6 [24], whereas others reported R_0 to be in the range of 2.2–3.1 [25] and, in Japan, 2.3 [13]. These estimated values of R_0 are reasonable for a community-wide setting and vary according to region. However, a school setting is different from a community-wide setting. It is a dense and close-contact setting. Hence, the virus transmission rate should be higher in a school setting. Paterson et al. used survey data from the students of the St. Francis Preparatory School outbreak to calculate the effective reproduction number R from the early growth rate of the epidemic in a school-based setting. This effective reproduction number R is usually comparable R_0 to in the early epidemic phase when all individuals can be considered susceptible. They reported that the basic reproduction number for this school-based setting is approximately 3.45 for an infectious period of 5 days [26].

We also calculated R_0 from epidemiological data obtained from the first school outbreak in Bangkok, Thailand. School *G* is the first school in Thailand in which the influenza A (H1N1) outbreak was detected. The number of daily laboratory-confirmed cases in the early epidemic phase is shown in Fig. 2. The basic reproduction number was estimated from the early epidemic phase in the absence of interventions, during which the effects of susceptible depletion are small [27]. After estimating the initial exponential growth rate (r) for the cumulative number of cases, the basic reproduction number was then computed by substituting r into the following expression [28,29]:

$$R_0 = \frac{R(t)}{S(t)},$$

where $R(t)$ is the effective reproduction number at time t, and $S(t)$ is the fraction of susceptible individuals at time t. If we consider only the early epidemic growth phase, the above equation can be simplified to [28]

$$R_0 = \frac{R(t \approx 0)}{S(t \approx 0)} = \frac{1 + Vr + f(1-f)(Vr)^2}{S(t \approx 0)} \approx 1 + Vr + f(1-f)(Vr)^2,$$

where V is the mean serial interval (the time between the onset of symptoms for the first generation and that for the second generation), and f is the ratio of the mean infectious period to the mean serial interval. The exponential growth rate, r, was found to be 0.2668 per day and the calculated R_0 was 3.58 (95% confidence interval: 2.88–4.28), which is close to the value found by [26] for a mean infectious period of 5 days and a mean incubation period of 2 days. We also calculated R_0 from data collected from jailed prisoners. A jail-based setting, like a school-based setting, is a close-contact setting. What we found was that in the jail-based setting, the R_0 was also greater than 3 (unpublished data), which confirms that in a

Table 1
Contact matrix. The contact numbers in the index-case floor are fitted with $y = 20\exp(-0.749x)$; the contact numbers between floors are fitted with $y = 36\exp(-0.723x)$ and are rounded to the nearest integer. Students in each room in the index-case floor are assumed to make the same contact number to other students in other floors. The label in Fig. 1(b) goes from left to right and top to bottom.

	Room1	Room2	Room3	Room4	Room5	Floor1	Floor2	Floor4	Floor5
Room1	20	9	4	2	1	8	17	17	8
Room2	9	20	9	4	2	8	17	17	8
Room3	4	9	20	9	4	8	17	17	8
Room4	2	4	9	20	9	8	17	17	8
Room5	1	2	4	9	20	8	17	17	8
Floor1	8	8	8	8	8	36	17	4	2
Floor2	17	17	17	17	17	17	36	8	4
Floor4	17	17	17	17	17	4	8	36	17
Floor5	8	8	8	8	8	2	4	17	36

close-contact setting the R_0 is usually high. We started this research work in June 2009, which was when the epidemic in Thailand just started, to give suggestions to the Royal Thai Government and policy makers how and when to close schools in Thailand; however, at that time, data concerning the number of infected students (and consequently R_0) in school G were not yet available. Therefore, in this study, unless stated otherwise, we use the value of R_0 from the literature: $R_0 = 3.45$ [26]. However, to investigate the (possible) uncertainty in R_0, we also performed a sensitivity analysis and ran simulations with various values of R_0. The results are shown in Section 3.5.

Eqs. (2.1)–(2.5) were numerically solved by using the explicit Euler method. We used a time step of $dt = 10^{-3}$ days; testing using a smaller time step did not change the result, and the integral was well converged. As expected from the simulations, there was only one infectious student in the index-case room, and the other students in the school were in the susceptible group. Afterward, the outbreak propagated in a wave-like manner.

2.2. Contact matrix, next generation matrix, and basic reproduction number

We employed a who-acquires-infection-from-whom matrix $\mathbf{M} = [M_{ij}]$, which gives the number of contacts of individuals from the ith compartment to the students in the jth compartment. A bi-directional contact pattern is assumed in this model, meaning that if the students in the ith compartment make n contacts with the students in the jth compartment, then the students in the jth compartment also make n contacts with the students in the ith compartment in a symmetrical manner. The transmission matrix $\boldsymbol{\beta} = [\beta_{ij}]$ is obtained by multiplying the contact matrix $\mathbf{M}$ with an appropriate scaling factor κ:

$$\boldsymbol{\beta} = \kappa\mathbf{M}. \tag{2.6}$$

The basic reproduction number R_0 is defined as the expected number of secondary infections produced by an index case in a completely susceptible population [23,27]. The next generation matrix in our model is the following:

$$\mathbf{N} = \boldsymbol{\beta}/\gamma = \kappa\mathbf{M}/\gamma. \tag{2.7}$$

The dominant eigenvalue of this matrix is defined as the basic reproduction number R_0 [23]. So our task is to find the scaling factor κ such that

$$R_0 = \max(\text{Eigenvalue}(\kappa\mathbf{M}/\gamma)). \tag{2.8}$$

Transmission between these spatial compartments is based on the contact matrix given in Table 1. We estimated the contact matrix by making the following assumptions: (1) In the index-case floor, a student can make 20 contacts with other students in the same room and 1 contact with other students in the room furthest away, while the contact pattern decreases exponentially across the room in the same floor (private communication). (2) Among floors, the contact pattern also decreases exponentially.

2.3. Non-pharmaceutical intervention strategies by school closure

We employed three non-pharmaceutical intervention strategies: (1) individual screening; (2) closure strategies: room, floor, or entire school closure; and (3) strategy (1) combined with strategy (2). With the individual screening strategy, symptomatic infectious students are allowed to stay at the school for a mean duration of T_a days after having developed into the infectious class (I); after this mean period of time, they are forced to stay at home and are moved to the recovered class (R), so they cannot infect other students anymore. We would like to emphasize that the school system was assumed to be a closed system. The closure strategy of rooms or floors was implemented by setting the transmission rate β_{ij} associated with rooms or floors to zero in the mean time interval of closure. This is because students in the closed rooms and floors cannot make any contact with other students in the school because they are forced to stay at home, so the contact rates must be zero. Similarly, the entire school closure strategy was implemented by setting all elements of the transmission rate matrix $\boldsymbol{\beta}$ to zero in the mean time interval of school closure.

3. Results and discussion

3.1. No intervention

We initially calculated the time course for the number of individuals in the S, E, A, I and R groups for the baseline scenario with no intervention strategy (Fig. 3). Because the proportion of the number of asymptomatic individuals to the number of total infectious individuals (C_A) remains uncertain for the H1N1 influenza, we used Thailand survey data, which found that C_A is about 0.3 (unpublished data). So, unless stated otherwise, we used $C_A = 0.3$. As shown in Fig. 3(a), the equilibrium value of recovered students was about 83%. This uncontrolled school epidemic "overshoots"; that is, more students are infected than the minimum percentage of immune individuals, $1 - 1/R_0 = 71\%$, needed to stop the epidemic in a perfectly mixed population. Fig. 3(b) shows the percentage of daily incidence for symptomatic infectious (I_{new}) and exposed (E_{new}) individuals. We can see that the peak value of I_{new} is 3.04% and occurs on the 24th day, and the peak value of E_{new} is 4.54% and occurs on the 22nd day, whereas the number of symptomatic infectious individuals I peaks on the 27th day, which lags slightly behind that of I_{new}, with a peak value of 12.85%. The percentage of infectious individuals in each room and floor were plotted as a function of time and shown in Fig. 3(c). From this figure, we can clearly see that the peaks of I for each room and floor occurred at different times. Students in rooms and floors that were close to the index-case room were infected faster than the ones that are far from the index-case room. The epidemic wave propagated from the index-case room to the room or floor furthest away, which was mainly driven by the contact matrix.

3.2. School closure strategies

In our work, we examined the effect of school closure on the course of an epidemic by subdividing the school closure strategy into closing only the index-case room, closing only the index-case floor, or closing the entire school. Fig. 4 shows the results of implementing the closure strategy in our school model. Note that, in our model, we have also isolated students from their communities, so when school is closed, all students are assumed to be quarantined to their homes. The graphs show the percentages of equilibrium-recovered individuals (R_{eq}) after implementing the strategy for (A) 5 days and (B) 9 days (other cases are shown in Section 3.5). From graphs (A) and (B), we can clearly see that with the same start date for implementing the intervention strategy, the entire school closure (SC) strategy was more effective than closing only the index-case floor (FC) or closing only the index-case room (RC). Moreover, the most effective date to start the closure strategy (RC, FC or SC) for both the 5-day closure and the 9-day closure was the 24th day. Interestingly, the 24th day was also the date with the peak number of daily incidences of infectious individuals (I_{new}). The entire school closure (SC) strategy reduced R_{eq} from 83% to 73.59% and 66.47% for the 5-day closure and the 9-day closure, respectively.

Our results are consistent with results from previous studies [19,30] that found that there is an optimal time to start the school closure strategy; moreover, our results suggest that the optimal time is the peak date of I_{new}. If we start to implement the closure strategy too early, there will be enough susceptible individuals left for the epidemic to resume when the control is lifted and when the school session is resumed. This can clearly be seen in Fig. 4(c), where we started to close the entire school for 9 days on the 18th day, which is before the optimal time (the 24th day). After the control was lifted, the epidemic resumed (as can be seen from the second peak). Our results, which show that there is an optimal time to start a school closure intervention, also agree with those reported by Bootsma and Ferguson [31]. They studied the effect of public health measures enacted in US cities during the 1918 influenza pandemic and reported that an optimal maximum effectiveness existed. They reported that effective control could reduce R_{eq} to 65%, while optimal control could reduce R_{eq} to 50% [31]. House et al. [20] also suggested that school closures should be timed to start just before the expected epidemic peak.

It should also be mentioned that deciding how long to close a school depends on many parameters (that are not considered here), e.g., mortality rate and disease severity. However, long-term school closure has an adverse economic impact; Sadique et al. [32] estimated a cost in the range of 0.2%–1.0% of GDP in the UK following 12 weeks of school closure. Lempel et al. [33] also estimated both the direct economic impact and health care impact for school closure durations of 2, 4, 6, and 12 weeks under a range of assumptions. They found that closing all schools in the US for 4 weeks could cost between \$10 and \$47 billion dollars (0.1%–0.3% of GDP) and lead to a reduction of 6%–19% in key health care personnel. Currently, there is no estimate of the economic impact of school closures in Thailand.

3.3. Individual screening strategy (IS)

Next, we examined an individual screening strategy (IS). In implementing this intervention strategy, symptomatic infectious students were allowed to stay at the school for a mean duration of T_a days after developing into the infectious class (I). After T_a days, they were forced to stay at home and were moved to the recovered class (R); hence, they could not further infect other students. Obviously, the efficiency of this intervention strategy depends on the asymptomatic proportion (AP or C_A), i.e., the proportion of asymptomatic infectious individuals to the total number of infectious individuals. If an epidemic has a higher AP, our ability to identify infectious students will be weakened (because we cannot identify students as infectious if they do not show any symptoms).

Fig. 5(a) shows the peak daily incidence values of symptomatic infectious individuals at various APs. Although, at the end, R_{eq} will be the same, the number of symptomatic infectious individuals at any time over the course of an epidemic

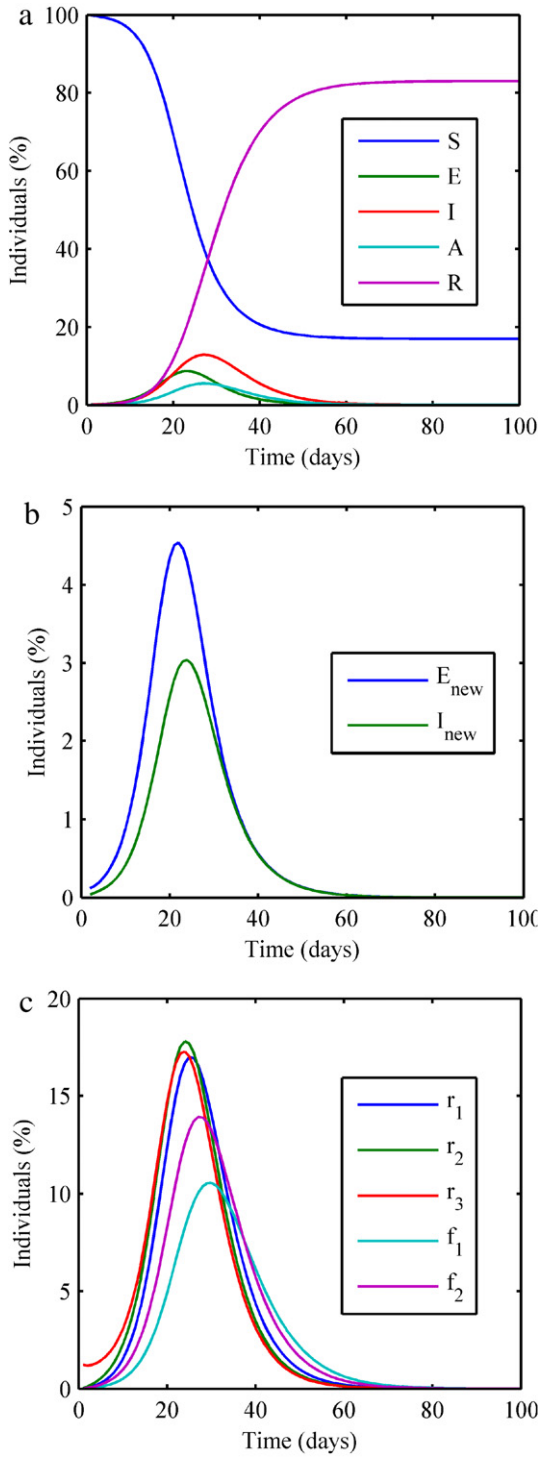

Fig. 3. Baseline results for no intervention. (a) Percentage of students in S, E, I, A, and R groups calculated from the entire school as a function of time (days). The asymptomatic proportion (C_A) $= 0.3$ was used. The steady state value of recovered students is about 83%. The peak of symptomatic infectious individuals occurs on the 27th day, with a peak value of 12.85%. (b) Percentage of daily incidences for symptomatic infectious (I_{new}) and exposed (E_{new}) individuals averaged over the entire school. The peak value of I_{new} is 3.04% and occurs on the 24th day, whereas the peak value of E_{new} is 4.54% and occurs on the 22nd day. On the 24th day, the cumulative number of symptomatic infectious individuals is 28%. (c) The percentage of infectious individuals in rooms 1, 2 and 3 (r_1, r_2 and r_3) from left to right on the index-case floor and floors 1 and 2 (f_1 and f_2). Note that r_3 is the index-case room.

is different for different APs. Implementing an IS strategy causes the contact patterns between students in the school to change. As a result, the peak date of I_{new} changes accordingly. Our peak dates of I_{new} as a function of T_a for various values of AP are shown in Fig. 5(b). We can see from the graph that the peak date of I_{new} shifted from the 24th day to a later day. The

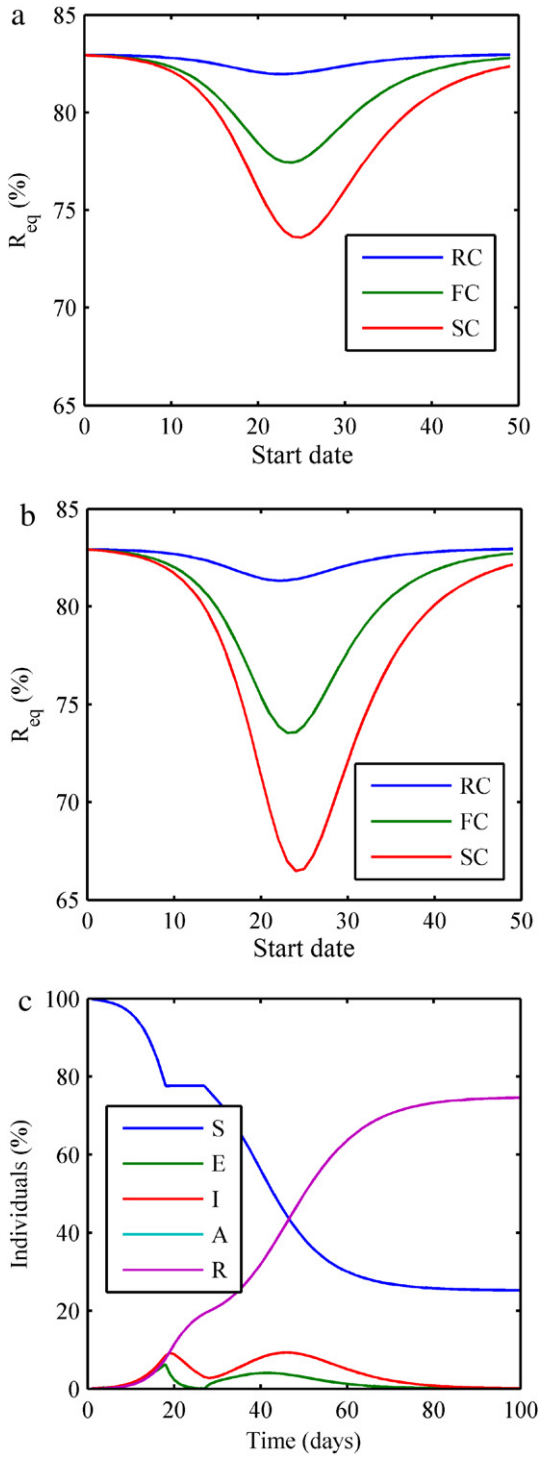

Fig. 4. The results of implementing the closure strategy alone. The graphs show the percentages of equilibrium-recovered individuals (R_{eq}) after implementing the strategy: closing only the index-case room (RC), closing only the index-case floor (FC), and closing the entire school (SC). The strategies were implemented for a time interval of 5 days (a) and 9 days (b). The x-axes show the start date of the closure strategy implementation. From both graphs, we can see that the entire school closure is the most effective intervention method in the closure category, and the 24th day is the most effective date to start to close the entire school for both the 5 day and 9 day closures. (c) Percentage of students in the S, E, I, A, and R groups calculated from the entire school as a function of time (days). The school closure started on the 18th day and lasted 9 days. From this figure, we can see that there are two peaks of I. The first peak occurs before the close date, while the other one occurs after the school classes have resumed. The steady state value of recovered students is about 75%.

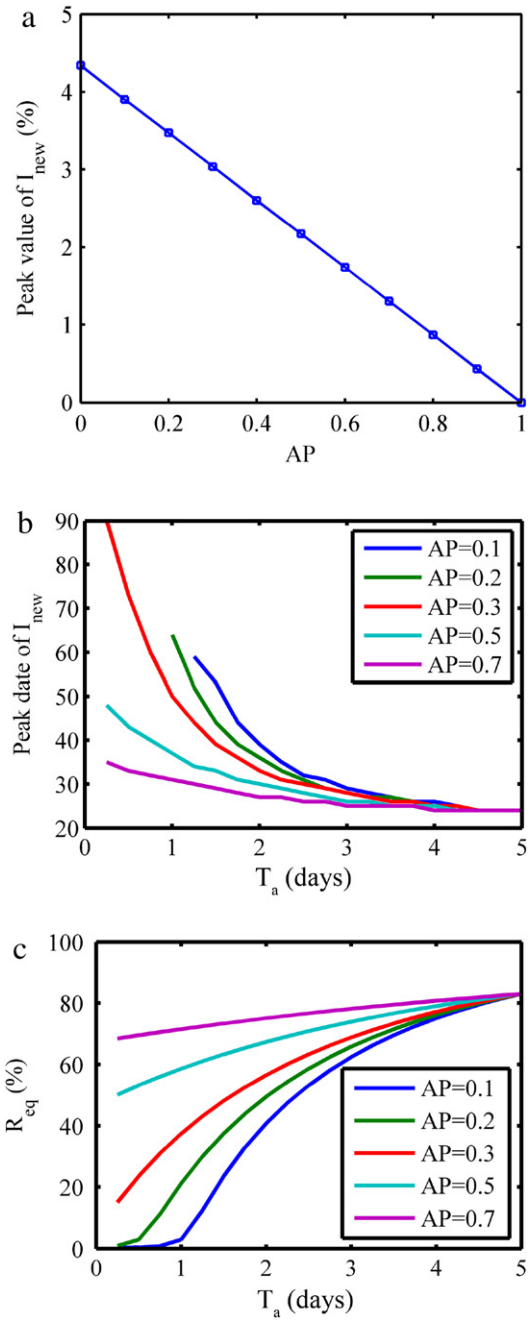

Fig. 5. The results of implementing the individual screening strategy (IS) alone. The individual screening strategy is stated at the beginning of the outbreak (time 0). (a) The peak value of the percentage of new daily symptomatic infectious cases (which is equal to $dI_{\text{cumulative}}/dt$ for $dt = 1$) at various asymptomatic proportions (APs). (b) The graph shows the date at which the peak value of I_{new} occurs versus the number of days in which symptomatic infectious students are allowed to stay at the school after they become infectious (T_a) for different numbers of APs. (c) The figure shows the percentage of the equilibrium-recovered individuals when the IS strategy is implemented with various T_a.

length of this shift depends on T_a and APs. The faster the T_a or the lower the AP, the longer the shift in peak date. This can be understood by considering that because the symptomatic infectious students are allowed to stay at the school only for T_a days, their infectious period is effectively equal to T_a days, which is usually shorter than the "real" infectious period of $1/\gamma$, and their reproduction number is thus reduced $T_a/(1/\gamma) = \gamma T_a$ times. The reduction in the reproduction number causes the epidemic to spread slower than in the uncontrolled case. Moreover, if the disease has a small AP, this will increase our effectiveness in identifying infectious students to force to stay at home and, therefore, the effectiveness of the IS strategy, which is consistent with the result from [19]. Lee et al. [19] found that when parents were able to identify and prevent 60% of symptomatic children from going to schools, the overall AR decreased from 34% to 29% and the peak of the epidemic was

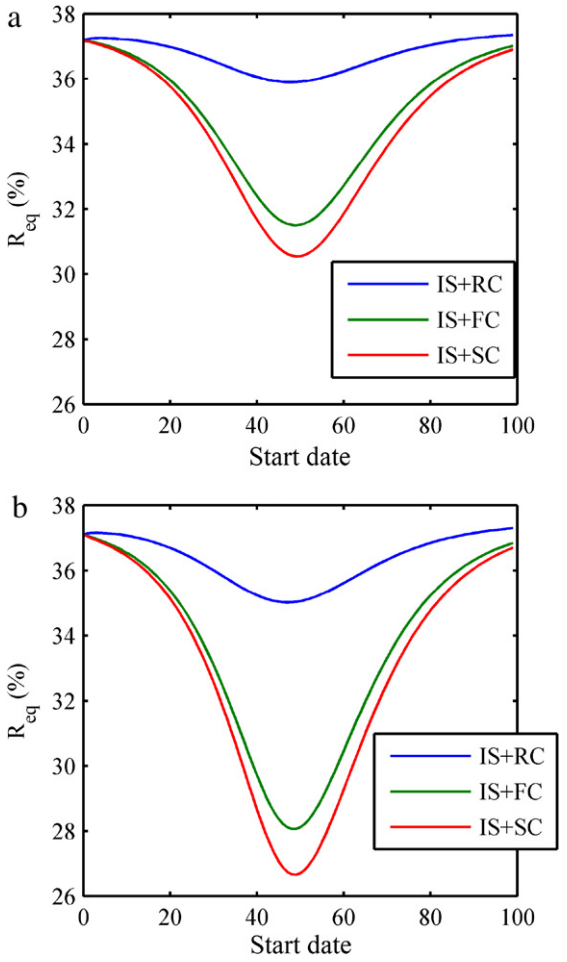

Fig. 6. The results of combining individual screening (IS) and closure strategies with $T_a = 1$. The IS was implemented from the start of the epidemic. The closure strategy started at various times. The close time interval is 5 days (a) and 9 days (b).

delayed by 1 week ($R_0 = 1.4$). However, our results ($R_0 = 3.45$) suggest that if the AP = 30% and if we are able to screen all infectious student with $T_a = 1$, the overall AR would decrease from approximately 83% to 40%, and the peak date could be delayed by approximately 4 weeks. This suggests that if we could isolate schools and students from their surrounding communities, the AR could be further reduced. The data for $T_a = 1$ and AP = 10% is absent because, at these parameter values, the epidemic dies out at the start. The number of equilibrium-recovered individuals (or cumulative patients) R_{eq} as a function of T_a after implementing the IS strategy is shown in Fig. 5(c). Apparently, R_{eq} strongly depends on T_a and AP. The faster the start time T_a and the lower the AP results, the lower the R_{eq}.

3.4. Individual screening strategy plus closure strategy

Finally, we combined the IS strategy with the closure strategy. The IS strategy started from time zero and was maintained indefinitely. The closure strategy started at varied times. Fig. 6 and Figure S1 (see Supplementary Information) show the results of the combined strategies for $T_a = 1$ and $T_a = 2$, respectively. The results suggest that the optimal time to start the closure strategy (either RC, FC, or SC) for $T_a = 1$ is the 49th day, when the cumulative number of symptomatic infectious individuals is 11.8%. However, the optimal time to start the closure strategy for $T_a = 2$ is the 32nd day, when the cumulative number of symptomatic infectious individuals is 16.8%. Again, these days are the peak dates of I_{new} for $T_a = 1$ and $T_a = 2$, respectively (see Fig. 5(b) for AP = 30%).

3.5. Sensitivity analysis (figures are shown in supplementary information)

As the epidemiological data for pandemic influenza are often uncertain, location specific, sparse, and limited, we additionally examined the sensitivity of our simulation results to 5 key model parameters, namely, the fraction of asymptomatic individuals (AP), the asymptomatic infectiousness (q), the basic reproduction number (R_0), the length of school closure, and the contact matrix.

Currently, there is no report for the value of q for the pandemic influenza A (H1N1), but some researchers estimate q to be 0.003 [21,22], while other works assume $q = 0.5$ [5,24,34–36]. In this work, we performed a sensitivity analysis

by varying q from 0.003 to 1. Jongcherdchootrakul et al. conducted surveys in school G and found that the asymptomatic proportion (AP) was about 30%. The value of the fraction of asymptomatic individuals in this work is based on the research by Kanlaya Jongcherdchootrakul et al. (First School Outbreak of Novel Influenza A (H1N1) Infections, Bangkok, June–August 2009), which is under the review process. However, other research works have assumed the AP to be 0.1, 0.36 and 0.5 [21,22], 0.33 [34], or 0.20 [35,36]. We performed a sensitivity analysis of the AP by varying the AP from 0.1 to 0.7. Uncertainty also remains for the value of the basic reproduction number; therefore, we also performed a sensitivity analysis of R_0 by varying R_0 from 1.2 to 5.0. Note that, unless otherwise stated, we used $R_0 = 3.45$, AP $= 0.3$, and $q = 1$.

Figure S2 and Figure S3 show the results when there are no intervention strategies. Figure S2 shows the sensitivity analysis for the peak date of I_{new}, the peak value of I_{new}, and the percentages of equilibrium-recovered individuals (R_{eq}) at various values of asymptomatic proportion (AP) and asymptomatic infectiousness (q) when there are no interventions. Clearly, the peak date of I_{new} is more shifted or delayed at the lower asymptomatic infectiousness and/or higher asymptomatic proportion (AP). This also causes a lower percentage of equilibrium-recovered individuals at the end of an epidemic. For large values of AP (e.g., AP > 0.7), the asymptomatic infectiousness parameter plays an important role in the model. Different values of q can give significantly different values for the final size of an epidemic and the peak date of I_{new} for a large AP. Obviously, when $q = 1$, both the peak date of I_{new} and R_{eq} do not depend on AP, and the peak value of I_{new} has a linear relationship with AP. There are no epidemics when $q < 0.003$, AP > 0.65 and $q < 0.25$, or AP > 0.85 for $R_0 = 3.45$.

In addition, Figure S3 shows the sensitivity analysis of the peak date of I_{new}, the peak value of I_{new}, and the percentages of equilibrium-recovered individuals (R_{eq}) as a function of the basic reproduction number (R_0) when there are no interventions. R_0 ranged from 1.2 to 5.0 with increments of 0.25, except for the first step, which had an increment of 0.3. The simulations were run with various values of asymptomatic infectiousness (q). From the figure, it can be seen that the peak of I_{new} appears earlier for a higher R_0 and/or q, and R_{eq} and the peak value of I_{new} are larger for a higher R_0 and/or q. We can also see that R_{eq} and the peak date of I_{new} with different values of q tend to converge to the same values at high R_0, whereas the peak value of I_{new} with different values of q tend to diverge at high R_0. This implies that the epidemics curve for higher values of q should be narrower. Note that there are no epidemics because the epidemics do not start when $R_0 \leq 1.5$, $q \leq 0.75$ and $R_0 \leq 1.75$, $q \leq 0.003$ for AP $= 0.3$.

The sensitivity analysis for the percentages of equilibrium-recovered individuals (R_{eq}) after implementing the entire school closure strategy (SC) for 9 days (without individual screening) as a function of the strategy start date for various values of asymptomatic infectiousness (q) and basic reproduction number (R_0) is shown in Figure S4(a) and (b). The optimum date to start the entire school closure strategy is when R_{eq} is at its minimum. We can clearly see that the optimum date is shifted to the right when the asymptomatic infectiousness and/or the basic reproduction number decreases. Moreover, R_{eq} also decreases when the asymptomatic infectiousness and/or the basic reproduction number decreases. Note that the results for implementing the entire school closure strategy alone do not depend on the asymptomatic proportion (AP) in our baseline case with $q = 1$. Figure S4(c) shows the optimum date for implementing the entire school closure strategy alone as a function of q. The solid line is the linear fit function $y = -10.02x + 33.82$, which gives an R-square of 0.995. Similarly, Figure S4(d) shows the optimum date for implementing the entire school closure strategy alone as a function of R_0. The solid line is the fit with the inverse-square function $y = 111.9x^{-2} + 14.46$, which gives an R-square of 0.9996.

Figure S5 and Figure S6 show the results when only the individual screening strategy (IS) is implemented. Figure S5 shows the sensitivity analysis for the peak date of I_{new} after implementing the individual screening strategy as a function of the time allowed at the school (T_a). In the simulations, T_a ranged from 0.25 to 5.0 in increments of 0.25. The results were obtained by varying values of the asymptomatic proportion (AP), asymptomatic infectiousness (q), and basic reproduction number (R_0). There were no well-defined peak dates of I_{new} in some parameter regimes at low values of T_a (indicated by the terminated line segments), which also implies that the epidemics cannot survive if we implement the IS strategy with these parameters. For example, if we know that an epidemic has $R_0 < 2.5$, $q = 1$ and AP $= 30\%$, we can stop it by implementing only the individual screening strategy with $T_a = 1$. Figure S6 shows the sensitivity analysis of the corresponding equilibrium-recovered individuals (R_{eq}) after implementing the individual screening strategy as a function of the time allowed at the school (T_a). It can clearly be seen from Figure S6(a) that the IS strategy is less effective when the epidemic has a higher AP, which is consistent with the results found by Lee et al. [19]. For example, for AP $= 0.7$, the IS strategy can reduce only about 10% (from 80% to 70%) of the R_{eq} with $T_a = 1$, whereas it can reduce almost 80% of R_{eq} with $T_a = 1$ if AP $= 0.1$. Moreover, from Figure S6(b), we can see that the reduction percentage of R_{eq} after implementing the IS strategy is less sensitive to the asymptomatic infectiousness (q). For $T_a = 1$, the IS strategy can roughly reduce the same amount of R_{eq} with different values of q. Similarly, Figure S6(c) implies that the IS strategy is less sensitive to the value of R_0, and, unless the epidemic goes extinct, the IS strategy can reduce approximately the same amount of R_{eq} with different values of R_0.

Figure S7 shows the sensitivity analysis for the percentages of equilibrium-recovered individuals (R_{eq}) after implementing the entire school closure strategy for 9 days together with an individual screening strategy with $T_a = 1$ day and as a function of the entire school closure start date for various values of (a) asymptomatic proportion (AP), (b) asymptomatic infectiousness (q), and (c) basic reproduction number (R_0). Note that the IS strategy was implemented at the start of the epidemic. We can see that, in general, the optimum date to start implementing the entire school closure strategy is shifted to the right when the asymptomatic proportion, the asymptomatic infectiousness, and/or the basic reproduction number decreases. R_{eq} also decreases when these parameters values decrease. However, there are some cases in which the optimum point to start the entire school closure is just at the start of the epidemic, e.g., figure (a) with AP $= 0.1$ and figure (b) with $q = 0.5$, and in some cases, there is no epidemic at all, e.g., figure (b) with $q < 0.25$ and figure (c) with

$R_0 < 2.0$. Implementing the IS strategy at the start of the epidemic should alter the contact pattern and lower the effective reproduction number. This also causes a shift and delay in the optimum time to start the entire school closure strategy (compared with Figure S4).

A sensitivity analysis of the percentages of equilibrium-recovered individuals (R_{eq}) when implementing the entire school closure strategy for 5 days, 9 days, 2 weeks, 8 weeks, and 16 weeks is shown in Figure S8. In figure (a), when the entire school closure strategy was implemented alone, we can see that doubling the closure interval from 4 weeks to 8 weeks and from 8 weeks to 16 weeks only slightly decreases R_{eq}. So, deciding how long to close school depends on many parameters (that are not considered here), e.g., mortality rate, disease severity, and economic costs. For the case of the influenza A (H1N1), the mortality rate and the severity of the disease is low [24,25], so closing the entire school for only 9 days or 2 weeks may be sufficient. Note that for the case of a closure interval of less than 2 weeks, the optimum date to start the entire school closure is the same, with a peak date of I_{new}. However, as the closure interval increased, the optimum date shifted slightly before the peak date of I_{new}. In figure (b), we implemented the IS strategy (at the start of the epidemic) together with the entire school closure strategy. Implementing the IS strategy further reduces the final number of infected individuals. Moreover, the long-duration SC (8 and 16 weeks) with the IS strategy can greatly enhance the reduction in R_{eq}. Similar to the case in figure (a), when the closure interval less than 2 weeks, the optimum date to start the entire school closure is still the same with a peak date of I_{new}.

Because there is currently no available data for the contact pattern of students in a school, in this section, we have also performed a sensitivity analysis by changing the contact pattern used in the simulations. Figure S9 shows the sensitivity analysis for the percentages of equilibrium-recovered individuals (R_{eq}) after implementing the entire school closure strategy alone (a) and together with the individual screening strategy with $T_a = 1$ day (b) for a closure interval of 2 weeks with various contact matrix patterns. First, we tried the linear function, which assumed that the relative contact frequency (y) linearly depends on the distance between rooms ($x = 0, 1, 2, 3, 4$), while the relative contact frequencies between students in the same room and the two farthest rooms were fixed at 20 and 1, respectively, so that the linear function for the index-case floor was $y_1 = -19x/4 + 20$ (the linear contact frequency function between floors can be found in the same manner). The second contact pattern was the exponential function, which has more compartment heterogeneity than our baseline contact pattern, $y_2 = 20\exp[-(\ln 40 + \ln 2)x/4 + \ln 2]$. The relative contact frequencies between students in the same room and between students in the two farthest rooms in this case were 40 and 0.5, respectively. The third pattern was the Gaussian function, $y_3 = 20\exp[-(\log 20)x^2/16]$, and the last one was the exponential function with twice the frequency of the baseline case; $y_4 = 40\exp(-0.749x)$. We can see from the figure that using different contact patterns only affects R_{eq} but not the characteristic of the results. Therefore, our conclusion that the optimum point to close the school is at or around the peak date of I_{new} is still valid and does not depend on the exact student contact pattern in the school. The y_4 curves are virtually the same as those of our baseline contact pattern (Figure S8). The more heterogeneous contact pattern (y_2) produces a lower R_{eq} compared to our baseline case. This is the obvious result because when there is more heterogeneity or locality, the disease is more likely to stay in the same compartment, thus causing a lower transmissivity.

4. Concluding remarks

Here, we employed the SEAIR model as an efficient numerical tool for simulating school closure to investigate what is the most effective criterion for conducting such a measure. Using data from initial outbreaks at School G in Bangkok, Thailand, from which detailed epidemiological data were collected, we estimated the basic reproduction number (R_0) to be 3.58 (95% confidence interval: 2.88–4.28). We tested various interventions, such as school closure and student screenings. It was found that closing the school on the peak date of the number of daily incidences appeared to be effective in preventing further outbreaks. Too early of a school closing resulted in subsequent episodes after reopening. Individual student screenings appeared to reduce the number of total cases by up to 40%. In a situation in which a widespread outbreak of a mild disease is unavoidable and in which the goal is to slowly reach sufficient herd immunity with a minimum number of cases, closing a school at the predicted peak date of the number of daily incidences plus screening for respiratory symptoms appears to be the most appropriate intervention method. Deciding how long to close the school depends on many parameters (that are not considered here), e.g., mortality rate and economic costs. For the case of influenza A (H1N1), the mortality rate and severity of the disease is low [24,25], and if we could isolate school and infectious individuals from communities, closing the entire school for only 9 days or 2 weeks with the individual screening strategy might be sufficient. Finally, we would like to mention that for a school closure intervention to work effectively, other interventions to control the spread of a pandemic should be simultaneously implemented, especially canceling large social gatherings or school events that are conducive to disease transmission.

Author disclosure statement

No competing financial interests exist.

Acknowledgments

The authors thank Mr. David Blyler for reading and editing the manuscript. Special thanks go to Associate Professors Prasit Palittapongarnpim, Sudarat Chadsuthi, Thitiwan Kerdsomboon, Monta Thammasatta, Sutheera Arjcharoen, and

Aungsuthorn Sirilaksanamanon for their fruitful discussion. This research project is supported by the Faculty of Science, Mahidol University, and the National Science and Technology Development Agency (NSTDA).

Appendix. Supplementary data

Supplementary material related to this article can be found online at doi:10.1016/j.mcm.2011.09.027.

References

[1] J.T. Wu, B.J. Cowling, E.H. Lau, D.K. Ip, L.M. Ho, T. Tsang, S.K. Chuang, P.Y. Leung, S.V. Lo, S.H. Liu, S. Riley, School closure and mitigation of pandemic (H1N1) 2009 Hong Kong, Emerg. Infect. Dis. 16 (3) (2010) 538–541.
[2] N.M. Ferguson, D.A. Cummings, S. Cauchemez, C. Fraser, S. Riley, A. Meeyai, S. Iamsirithaworn, D.S. Burke, Strategies for containing an emerging influenza pandemic in Southeast Asia, Nature 437 (7056) (2005) 209–214.
[3] N.M. Ferguson, D.A. Cummings, C. Fraser, J.C. Cajka, P.C. Cooley, D.S. Burke, Strategies for mitigating an influenza pandemic, Nature 442 (7101) (2006) 448–452.
[4] T.C. Germann, K. Kadau, I.M. Longini Jr., C.A. Macken, Mitigation strategies for pandemic influenza in the United States, Proc. Natl. Acad. Sci. USA 103 (15) (2006) 5935–5940.
[5] I.M. Longini Jr., A. Nizam, S. Xu, K. Ungchusak, W. Hanshaoworakul, D.A. Cummings, M.E. Halloran, Containing pandemic influenza at the source, Science 309 (5737) (2005) 1083–1087.
[6] L.O. Gostin, Pandemic influenza: public health preparedness for the next global health emergency, J. Law Med. Ethics 32 (4) (2004) 565–573.
[7] R. Gani, H. Hughes, D. Fleming, T. Griffin, J. Medlock, S. Leach, Potential impact of antiviral drug use during influenza pandemic, Emerg. Infect. Dis. 11 (9) (2005) 1355–1362.
[8] K. Stohr, M. Esveld, Public health. Will vaccines be available for the next influenza pandemic? Science 306 (5705) (2004) 2195–2196.
[9] I.M. Longini Jr., M.E. Halloran, Strategy for distribution of influenza vaccine to high-risk groups and children, Am. J. Epidemiol. 161 (4) (2005) 303–306.
[10] S. Cauchemez, N.M. Ferguson, C. Wachtel, A. Tegnell, G. Saour, B. Duncan, A. Nicoll, Closure of schools during an influenza pandemic, Lancet Infect. Dis. 9 (8) (2009) 473–481.
[11] S. Cauchemez, A.J. Valleron, P.Y. Boelle, A. Flahault, N.M. Ferguson, Estimating the impact of school closure on influenza transmission from Sentinel data, Nature 452 (7188) (2008) 750–754.
[12] K. Glass, B. Barnes, How much would closing schools reduce transmission during an influenza pandemic? Epidemiology 18 (5) (2007) 623–628.
[13] H. Nishiura, C. Castillo-Chavez, M. Safan, G. Chowell, Transmission potential of the new influenza A(H1N1) virus and its age-specificity in Japan, Eurosurveillance 14 (22) (2009).
[14] K. Jongcherdchootrakul, R. Sukkawee, K. Khaoprawet, J. Silaporn, S.R. Wattanarungsan, P. Ayood, S. Iamsirithaworn, P. Siriarayapon, First school outbreak of novel influenza A (H1N1) infection in Thailand, Weekly Epidemiology Surveillance Report 412009 49–56, June–August 2009.
[15] S. Santayakorn, C. Pittayawonganon, P. Thammavijaya, W. Sitthi, V. Wongphruksasoog, S. Al-sihak, B. Ardkam, N. Prajaksub, A. Kanchanapiboonwong, P. Ayood, C. Daraphong, P. Silaporn, H. Kanchanasombat, N. Trichaisri, P. Krongyat, R. Kritsanasap, Investigation of influenza A H1N1 outbreak in school A, Angthong, August 2009, Weekly Epidemiology Surveillance Report, 40 (665-8) 2009.
[16] H.P. Duerr, S.O. Brockmann, I. Piechotowski, M. Schwehm, M. Eichner, Influenza pandemic intervention planning using InfluSim: pharmaceutical and non-pharmaceutical interventions, BMC Infect. Dis. 7 (76) (2007).
[17] M. Eichner, M. Schwehm, H.P. Duerr, S.O. Brockmann, The influenza pandemic preparedness planning tool InfluSim, BMC Infect. Dis. 7 (17) (2007).
[18] S. Mniszewski, S. Del Valle, P. Stroud, J. Riese, S. Sydoriak, EpiSimS simulation of a multi-component strategy for pandemic influenza, in: 2008: The Society for Computer Simulation, International.
[19] B.Y. Lee, S.T. Brown, P. Cooley, M.A. Potter, W.D. Wheaton, R.E. Voorhees, S. Stebbins, J.J. Grefenstette, S.M. Zimmer, R. Zimmerman, Simulating school closure strategies to mitigate an influenza epidemic, J. Public Health Manag. Pract. JPHMP 16 (3) (2010) 252.
[20] T. House, M. Baguelin, A.J. Van Hoek, P.J. White, Z. Sadique, K. Eames, J.M. Read, N. Hens, A. Melegaro, W.J. Edmunds, Modelling the impact of local reactive school closures on critical care provision during an influenza pandemic, Proc. R. Soc. Biol. Sci. Ser. B (2011).
[21] S. Lee, G. Chowell, C. Castillo-Chávez, Optimal control for pandemic influenza: the role of limited antiviral treatment and isolation, J. Theoret. Biol. 265 (2) (2010) 136–150.
[22] G. Chowell, C.E. Ammon, N.W. Hengartner, J.M. Hyman, Transmission dynamics of the great influenza pandemic of 1918 in Geneva, Switzerland: assessing the effects of hypothetical interventions, J. Theoret. Biol. 241 (2) (2006) 193–204.
[23] O. Diekmann, J. Heesterbeek, Mathematical Epidemiology of Infectious Diseases: Model Building, Analysis, and Interpretation, Wiley, 2000.
[24] C. Fraser, C.A. Donnelly, S. Cauchemez, W.P. Hanage, M.D. Van Kerkhove, T.D. Hollingsworth, J. Griffin, R.F. Baggaley, H.E. Jenkins, E.J. Lyons, T. Jombart, W.R. Hinsley, N.C. Grassly, F. Balloux, A.C. Ghani, N.M. Ferguson, A. Rambaut, O.G. Pybus, H. Lopez-Gatell, C.M. Alpuche-Aranda, I.B. Chapela, E.P. Zavala, D.M. Guevara, F. Checchi, E. Garcia, S. Hugonnet, C. Roth, Pandemic potential of a strain of influenza A (H1N1): early findings, Science 324 (5934) (2009) 1557–1561.
[25] P.Y. Boelle, P. Bernillon, J.C. Desenclos, A preliminary estimation of the reproduction ratio for new influenza A(H1N1) from the outbreak in Mexico, March–April 2009, Euro. Surveill. 14 (19) (2009).
[26] B. Paterson, D.N. Durrheim, F. Tuyl, Influenza: H1N1 goes to school, Science 325 (5944) (2009) 1071–1072. Author reply 1072-3.
[27] R. Anderson, R. May, Infectious Diseases of Humans: Dynamics and Control, Oxford Univ. Press, New York, 1991, 757.
[28] M. Lipsitch, T. Cohen, B. Cooper, J.M. Robins, S. Ma, L. James, G. Gopalakrishna, S.K. Chew, C.C. Tan, M.H. Samore, D. Fisman, M. Murray, Transmission dynamics and control of severe acute respiratory syndrome, Science 300 (5627) (2003) 1966–1970.
[29] C. Jackson, E. Vynnycky, P. Mangtani, Estimates of the transmissibility of the 1968 (Hong Kong) influenza pandemic: evidence of increased transmissibility between successive waves, Am. J. Epidemiol. 171 (4) (2010) 465.
[30] N. Halder, J.K. Kelso, G.J. Milne, Developing guidelines for school closure interventions to be used during a future influenza pandemic, BMC Infect. Dis. 10 (2010) 221.
[31] M.C. Bootsma, N.M. Ferguson, The effect of public health measures on the 1918 influenza pandemic in US cities, Proc. Natl. Acad. Sci. USA 104 (18) (2007) 7588–7593.
[32] M.Z. Sadique, E.J. Adams, W.J. Edmunds, Estimating the costs of school closure for mitigating an influenza pandemic, BMC Public Health 8 (1) (2008) 135.
[33] H. Lempel, J.M. Epstein, R.A. Hammond, Economic cost and health care workforce effects of school closures in the US PLoS currents, 12009.
[34] D. Balcan, H. Hu, B. Goncalves, P. Bajardi, C. Poletto, J.J. Ramasco, D. Paolotti, N. Perra, M. Tizzoni, W.V.D. Broeck, V. Colizza, A. Vespignani, Seasonal transmission potential and activity peaks of the new influenza A (H1N1): a Monte Carlo likelihood analysis based on human mobility, BMC Med. 7 (2009) 45.
[35] N. Halder, J.K. Kelso, G.J. Milne, Developing guidelines for school closure interventions to be used during a future influenza pandemic, BMC Infect. Dis. 10 (2009).
[36] N. Halder, J.K. Kelso, G.J. Milne, Analysis of the effectiveness of interventions used during the 2009 A/H1N1 influenza pandemic, BMC Public Health 10 (168) (2010).